Kinetics of GLUT4 Trafficking in Rat and Human Skeletal Muscle

Håkan K.R. Karlsson,[1] Alexander V. Chibalin,[1] Heikki A. Koistinen,[1,2,3] Jing Yang,[4] Francoise Koumanov,[4] Harriet Wallberg-Henriksson,[5] Juleen R. Zierath,[1] and Geoffrey D. Holman[4]

OBJECTIVE—In skeletal muscle, insulin stimulates glucose transport activity three- to fourfold, and a large part of this stimulation is associated with a net translocation of GLUT4 from an intracellular compartment to the cell surface. We examined the extent to which insulin or the AMP-activated protein kinase activator AICAR can lead to a stimulation of the exocytosis limb of the GLUT4 translocation pathway and thereby account for the net increase in glucose transport activity.

RESEARCH DESIGN AND METHODS—Using a biotinylated photoaffinity label, we tagged endogenous GLUT4 and studied the kinetics of exocytosis of the tagged protein in rat and human skeletal muscle in response to insulin or AICAR. Isolated epitrochlearis muscles were obtained from male Wistar rats. Vastus lateralis skeletal muscle strips were prepared from open muscle biopsies obtained from six healthy men (age 39 ± 11 years and BMI 25.8 ± 0.8 kg/m^2).

RESULTS—In rat epitrochlearis muscle, insulin exposure leads to a sixfold stimulation of the GLUT4 exocytosis rate (with basal and insulin-stimulated rate constants of 0.010 and 0.067 min^{-1}, respectively). In human vastus lateralis muscle, insulin stimulates GLUT4 translocation by a similar sixfold increase in the exocytosis rate constant (with basal and insulin-stimulated rate constants of 0.011 and 0.075 min^{-1}, respectively). In contrast, AICAR treatment does not markedly increase exocytosis in either rat or human muscle.

CONCLUSIONS—Insulin stimulation of the GLUT4 exocytosis rate constant is sufficient to account for most of the observed increase in glucose transport activity in rat and human muscle.
***Diabetes* 58:847–854, 2009**

Impairments in skeletal muscle glucose uptake occur in type 2 diabetes (1–4) and are associated with defects in GLUT4 translocation rather than a change in the total amount of GLUT4 protein (2,5). These changes are also associated with defects in cell signaling (6,7). However, in healthy normal glucose-tolerant relatives of type 2 diabetic patients, impairments in skeletal muscle insulin-stimulated glucose transport activity occur without alterations in the phosphorylation of Akt or its downstream target protein AS160 (8). In rodents, marked impairments in insulin signaling to glycogen metabolism occur as a consequence of skeletal muscle GLUT4 knockout (9), suggesting that defects in GLUT4 traffic have the potential to feed back and inhibit early steps in insulin signaling. Changes in GLUT4 translocation may be one of the earliest molecular defects in type 2 diabetes (8). Thus, it is important to determine molecular mechanisms that link insulin signaling to GLUT4 translocation.

Skeletal muscle represents the major site of postprandial glucose disposal (10); therefore, kinetic studies of GLUT4 trafficking in this tissue are important to determining the major sites of insulin action, particularly because GLUT4-trafficking defects have been observed in skeletal muscle from type 2 diabetic patients (11,12). In adipose tissue, GLUT4-trafficking kinetic studies have identified the exocytic limb of the translocation pathway as the major site of insulin action (13–16). In contrast to adipocytes, skeletal muscle is a complex tissue, with diverse GLUT4 storage sites, including multiple perinuclear and satellite compartments that are close to the transverse tubules (17–19). Moreover, skeletal muscle GLUT4 translocation and glucose transport are increased in response to a wide range of stimulatory factors including contraction, changes in calcium release, and changes in the cellular energy status and AMP levels (19).

To determine the extent to which insulin action stimulates the exocytosis limb of the GLUT4 translocation pathway, and thereby account for the net increase in translocation, we have developed new methods for studying GLUT4 translocation in rat epitrochlearis and human vastus lateralis skeletal muscle. We have specifically examined whether the stimulation of exocytosis following exposure to insulin or the AMP precursor analogue AICAR (5-aminoimidazole-4-carboxamide ribonucleoside) can fully account for associated increases in glucose transport activity.

From the [1]Department of Molecular Medicine and Surgery, Karolinska Institutet, Stockholm, Sweden; the [2]Department of Medicine, Division of Cardiology, Helsinki University Central Hospital, Helsinki, Finland; the [3]Minerva Foundation Institute for Medical Research, Biomedicum 2U Helsinki, Helsinki, Finland; the [4]Department of Biology and Biochemistry, University of Bath, Bath, U.K.; and the [5]Department of Physiology and Pharmacology, Karolinska Institutet, Stockholm, Sweden.

Corresponding author: Geoffrey D. Holman, g.d.holman@bath.ac.uk.

Received 5 November 2008 and accepted 19 January 2009.

Published ahead of print at http://diabetes.diabetesjournals.org on 2 February 2009. DOI: 10.2337/db08-1539.

RESEARCH DESIGN AND METHODS

Epitrochlearis muscle isolation. Male Wistar rats (150–200 g) were obtained from B&K Universal, Sollentuna, Sweden. Animals were housed under a 12-h light/12-h dark cycle and had free access to water and standard rodent chow and were fasted (5 h) before each experiment. The Stockholm North Animal Ethics Committee approved all studies. Rats were anesthetized with an intraperitoneal injection of sodium pentobarbital (5 mg/100 g body wt i.p.). Isolated epitrochlearis muscles were incubated at 30°C. All incubation media were prepared from pregassed (95% O_2/5% CO_2) Krebs-Henseleit buffer (KHB) containing 5 mmol/l HEPES and 0.1% BSA (radioimmunoassay grade). The gas phase in the vials was maintained at 95% O_2/5% CO_2.

Open muscle biopsy. Six healthy men with no known family history of metabolic disorder (aged 39 ± 11 years and BMI 25.8 ± 0.8 kg/m^2) volunteered for the muscle biopsy procedure. All subjects were instructed to avoid strenuous exercise for 72 h before the muscle biopsy. The subjects reported to the laboratory after an overnight fast. The study protocol was approved by

the ethics committee of the Karolinska Institutet, and informed consent was received from all subjects before participation.

Open biopsies were taken from vastus lateralis muscle under local anesthesia (5 mg/ml mepivakain chloride), as previously described (20,11). Muscle strips were dissected, mounted on Plexiglass clamps, and incubated in vitro in pregassed (95% O_2 and 5% CO_2) KHB in a shaking water bath at 35°C.

Glucose transport. Isolated rat epitrochlearis muscles were incubated in pregassed KHB containing 15 mmol/l mannitol and 5 mmol/l glucose for 20 min. Muscles were transferred to fresh KHB and incubated with either 120 nmol/l insulin or 1 mmol/l AICAR for the times specified in the figure legends. Muscles were then transferred to fresh KHB containing 20 mmol/l mannitol and incubated for 10 min to rinse excess glucose, followed by incubation for 12 min in KHB containing 5 mmol/l 3-O-methyl-D-[^{3}H]-glucose (800 μCi/mmol) and 15 mmol/l [^{14}C]-mannitol (53 μCi/mmol). Muscles were blotted of excess fluid, frozen in liquid nitrogen, and stored at −80°C. Glucose transport rate was analyzed by the accumulation of intracellular 3-O-methyl [^{3}H] glucose (21).

Akt and AMP-activated protein kinase phosphorylation. Muscles were homogenized and protein phosphorylation was determined as previously described (22) by Western blot analysis using anti–phospho-Ser473 Akt, anti–phospho-Thr172 AMP-activated protein kinase (AMPK)-α, or anti–phospho-Ser79 acetyl CoA carboxylase antibodies (from Cell Signaling Laboratories).

GP15 photoaffinity tagging of GLUT4. A biotin tag was introduced into GLUT4 using a photolabeling procedure. Muscles were incubated at 18°C for 8 min in the presence of 1 mmol/l glucose-photolabel-15 (GP15) (23,24) and then irradiated for 2 min in a Rayonet photochemical reactor (Southern New England Ultraviolet, Branford, CT) using 300-nm lamps. Muscles were rinsed four times in ice-cold PBS and either frozen directly in liquid nitrogen or transferred for continued incubation. Muscles were stored at −80°C until analysis. GP15-tagged GLUT4 was identified as described (12) for the similar but shorter photoaffinity labeling compound Bio-LC-ATB-BMPA.

Steady-state internalization of GLUT4. For internalization-trafficking time course experiments, rat epitrochlearis muscles were first incubated in KHB containing 15 mmol/l mannitol and 5 mmol/l glucose at 30°C for 20 min. Muscles were then transferred to fresh KHB and incubated with either 120 nmol/l insulin for 30 min or 1 mmol/l AICAR for 50 min. Insulin and AICAR concentrations were maintained at these constant levels throughout the remainder of the protocol. Before GP15 photoaffinity tagging of GLUT4, muscles were transferred to fresh KHB containing 20 mmol/l mannitol for 10 min to rinse away glucose. KHB was cooled to 18°C during photoaffinity tagging to slow transporter recycling.

After irradiation, muscles were washed once in KHB at 18°C to remove excess GP15 label and were then transferred to fresh KHB and incubated at 30°C to initiate internalization of the biotin-tagged GLUT4. At the specified internalization time points, 80 μg/ml avidin (Pierce Chemical, Rockford, IL) was added for 6 min at 30°C to block transporters that were still at the cell surface. Muscles were rinsed four times in ice-cold PBS, frozen directly in liquid nitrogen, and stored at −80°C until analysis. The maximum signal of GLUT4, which internalized and escaped the surface quenching, was determined in each experiment from insulin- or AICAR-stimulated samples that were returned to the basal state and allowed to internalize the biotinylated GLUT4 for 60 min. Initial GLUT4 signal was determined in samples incubated without the addition of avidin.

Exocytosis of GLUT4. For exocytosis experiments, human vastus lateralis muscles or rat epitrochlearis muscles were incubated at 35 or 30°C, respectively. After 20 min, muscles were transferred to fresh KHB containing 12 nmol/l insulin. Insulin-stimulated muscles were photoaffinity labeled with GP15 and subsequently washed with MES buffer (KHB with MES replacing HEPES), pH 6.0, for 5 min to terminate insulin stimulation. Muscles were maintained in KHB for 40 min to obtain maximal internalization. To begin the determination of exocytosis, 160 μg/ml avidin was added for 6 min. Thereafter, muscles were transferred to KHB with or without 120 nmol/l insulin or 1 mmol/l AICAR for specified times. The rate of loss of the internal transporters as they became quenched by the surface avidin was determined at the indicated time points.

Curve fitting and analysis of rate constants. Values for net internalization of GLUT4 under steady-state conditions were curve fitted using a two-parameter equation: $F = (1.0 - E).\exp(-k.t) + E$, where F is the fraction of GLUT4 remaining at the surface, E is the equilibrium position for internalization, k is the net internalization–rate constant, and t is time. The contributions from exocytosis (kex) and endocytosis (ken) to the progress to equilibrium were determined using the following equation: $F = \{\text{kex} + \text{ken}.\exp[-\text{t}.(\text{kex} + \text{ken})]\}/(\text{kex} + \text{ken})$ (11). Values for unidirectional exocytosis of GLUT4 were curve fitted to a single exponential equation: $F = \exp(-k.t)$, where F is the fraction of GLUT4 remaining internal, and k is the exocytosis rate constant, and t is time. Individual experiments were analyzed, and the resulting parameters were used to obtain mean and SE values, which were then compared in unpaired t tests. Differences were considered significant at $P < 0.05$. Analysis and curve fitting were carried out using Graphpad Prism software.

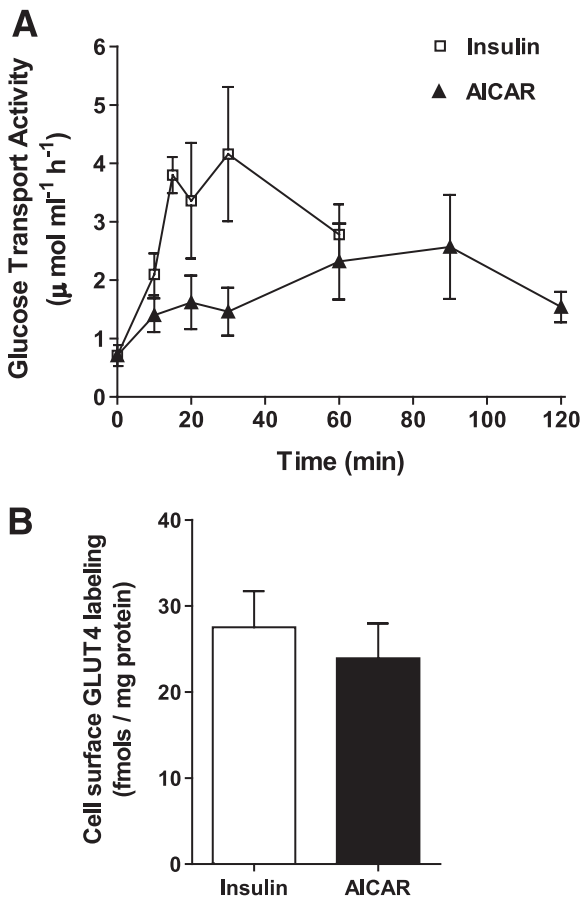

FIG. 1. Comparison of the stimulation of glucose transport and cell-surface GLUT4 levels by insulin and AICAR in rat epitrochlearis muscle. *A*: Transport rates were determined from measurements of 3-O-methyl-D-[^{3}H]-glucose uptake into muscle specimens incubated for the indicated times in the presence of 120 nmol/l insulin or 1 mmol/l AICAR. Results are means ± SE of six experiments. *B*: Levels of cell surface GLUT4 were determined by labeling muscle strips with GP15 photolabel following 30 min of incubation with 120 nmol/l insulin (■) and 50 min of incubation with 1 mmol/l AICAR (□). Labeled samples were solubilized, and the biotin-tagged GLUT4 was precipitated on immobilized streptavidin, resolved on SDS-PAGE gels, and then detected and quantified by blotting with GLUT4 antibody. Results are means ± SE of six (insulin) and five (AICAR) experiments.

RESULTS

Comparison of insulin and AICAR treatment on glucose transport activity in rat epitrochlearis muscle. Insulin stimulation of epitrochlearis muscle leads to a rapid increase in glucose transport activity that reaches an equilibrium level of stimulation three- to fourfold above basal levels within 20 min (Fig. 1*A*). Conversely, in response to AICAR, the maximum level of stimulation is slower in onset and only reaches a level of stimulation ~2.5-fold above basal after 60 min. The maximum levels of stimulation by insulin and AICAR are maintained at a steady state for a further 30 min. At the steady state, the stimulation of glucose transport activity by insulin is slightly higher than that induced by AICAR. We assessed whether changes in the kinetics of GLUT4 trafficking induced by these treatments could account for the differences observed in glucose transport activity. We used an

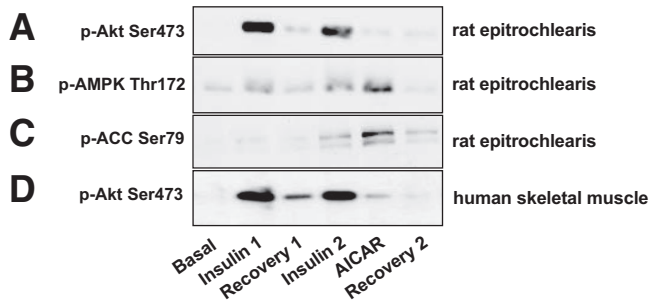

FIG. 2. Phospho-protein signaling in rat epitrochlearis and human vastus lateralis muscle. Immunoblots of *p*–Akt Ser473 (*A*), *p*–AMPK Thr172 (*B*), and *p*–CoA carboxylase Ser79 (*C*) in lysates of rat epitrochlearis and *p*–Akt Ser 473 (*D*) in human vastus lateralis muscle. Muscle lysates were resolved on SDS-PAGE, transferred to nitrocellulose membranes, and incubated overnight with phospho-specific antibodies. Immunoreactive proteins were visualized by enhanced chemiluminescence. Conditions are as follows: basal, initial basal; insulin 1, 12 nmol/l insulin stimulation for 52 min; recovery 1, 102-min recovery after removal of initial insulin stimulation; insulin 2, restimulation with 120 nmol/l insulin for 50 min after recovery; AICAR, restimulation with 1 mmol/l AICAR for 50 min after recovery; and recovery 2, 162-min recovery after removal of initial insulin stimulation. The figure includes representative immunoblots from six independent experiments.

impermeable probe (GP15) to tag GLUT4 transporters at the cell surface. GP15 consists of a glucose moiety that is recognized by the GLUT4 binding site and a biotin tag that can interact with avidin or streptavidin. The biotin and glucose moieties are separated by a very long spacer that allows access of avidin to the tagged transporter (23,24). We found that the higher increase in glucose transport activity following insulin stimulation versus AICAR stimulation is matched by a slightly but insignificantly higher level of steady-state GLUT4 labeling by GP15 (Fig. 1*B*).

In addition to the observed differences in the rate of onset of the maximal stimulation of glucose transport activity, insulin and AICAR produce a markedly different pattern of early signaling changes in the intermediate serine kinases, Akt/protein kinase B, and AMPK. Insulin, but not AICAR, action leads to a marked stimulation of Akt phosphorylation (Fig. 2*A*). Conversely, AICAR, but not insulin, action leads to a robust stimulation of AMPK phosphorylation (Fig. 2*B*) and the downstream AMPK substrate acetylCoA carboxylase (Fig. 2*C*). The slight increase in AMPK phosphorylation following insulin treatment is not significant over a series of experiments or when corrected for total AMPK levels. The maximally rapid time frame for insulin-stimulated increase in Akt phosphorylation was within 2–10 min, and the AICAR-stimulated increase in AMPK phosphorylation also occurred rapidly and reached a maximum within 30 min (25) (H.K.R.K., A.V.C., H.A.K., J.Y., F.K., H.W.-H., J.R.Z., G.D.H., unpublished data). This increase is more rapid than the increase to maximal levels of glucose transport activity (Fig. 1*A*).

Steady-state GLUT4 trafficking in insulin- and AICAR-stimulated rat epitrochlearis muscle. The maintenance of steady-state and maximal levels of glucose transport activity and cell-surface GLUT4 content (Fig. *1*) could be due to a pulse of GLUT4 translocation, which is then followed by a cessation of subsequent movement as the cell signaling processes continue. Alternatively, GLUT4 could continue to recycle under steady-state conditions, and the cell-surface GLUT4 level could be maintained by a net balance of a fast exocytosis and a fast endocytosis rate of translocation. In adipocytes, GLUT4 appears to continuously recycle during insulin-stimulated signaling (13,26,27). Therefore, we determined whether GLUT4 continues to recycle in rat skeletal muscle. The rate of net internalization of GP15-tagged GLUT4 under steady-state stimulation by either insulin or AICAR has been measured by separating the GLUT4 that remains at the cell surface from that which has been internalized. To do this, avidin is added to the muscle specimens after labeling. The initial cell-surface labeling (first lane in Fig. 3*A*) is reduced by the avidin addition at the beginning of the time course (second lane in Fig. 3*A*). At subsequent times of incubation, GLUT4 internalizes and escapes the extracellular avidin. This gives a steady rise in the internal signal from the tagged GLUT4 at 5–60 min (Fig. 3*A*). The steady-state insulin stimulation is associated with rapid internalization that is almost complete within 10 min. The final level of net internalization occurs when approximately half the initial cell-surface GLUT4 is internalized (Fig. 3*B*). At this point, the exocytosis and endocytosis are balanced to maintain the surface levels of GLUT4. Conversely, the steady-state AICAR stimulation is associated with a slower initial net internalization, particularly over the first 5 min where the fraction of internalization is lower than that occurring in insulin-stimulated muscle. Additionally, the rate of progress to the equilibrium level is not complete until 30–60 min (Fig. 3*B*). This is associated with a slower rate constant for net internalization between AICAR- and insulin-stimulated muscles (0.059 vs. 0.134 min^{-1}, respectively). Furthermore, the final equilibrium level of internalized GLUT4 is reached at a lower cell-surface fraction (0.29) than that associated with insulin stimulation (0.52) (Fig. 3*C*). Further analysis of the steady-state data (Fig. 3*D*) indicates that AICAR treatment is associated with a slower endocytosis rate constant (0.042 vs. 0.068 min^{-1}) and a much slower exocytosis rate constant (0.017 vs. 0.067 min^{-1}). These kinetic parameters predict that the levels of glucose transport activity and cell-surface GLUT4 in AICAR-treated muscle will be 55% of those in insulin-treated muscle. These values are in reasonable agreement with data presented in Fig. 1.

The steady-state data reveal important differences in the kinetics of GLUT4 trafficking following insulin or AICAR treatment. However, the net internalization of GLUT4 under these conditions is a complex kinetic process that involves both endocytosis of GLUT4 and its recycling (exocytosis). To further address whether AICAR- or insulin-stimulated glucose transport and signaling activities occur by a convergent mechanism, we simplified our study design in subsequent experiments to only measure the exocytosis rate constant.

Exocytosis of GLUT4 in insulin- and AICAR-stimulated rat epitrochlearis muscle. To more directly measure the kinetic parameters of exocytosis, a procedure was adopted in which GP15-tagged GLUT4 was internalized and then the unidirectional return to the cell surface was monitored. To internalize the GP15-tagged GLUT4, it was necessary to first label insulin-stimulated muscle and then reverse the stimulated state by washing with a low pH buffer that disassociates insulin from its receptor (28). To check that this procedure is adequately effective, we monitored the reversal of Akt phosphorylation (Fig. 2*A*). Akt phosphorylation is reduced toward basal levels within 100 min. The return to basal levels of phosphorylation is incomplete; however, it is only necessary that the reversal process is sufficient to allow a detectable portion of

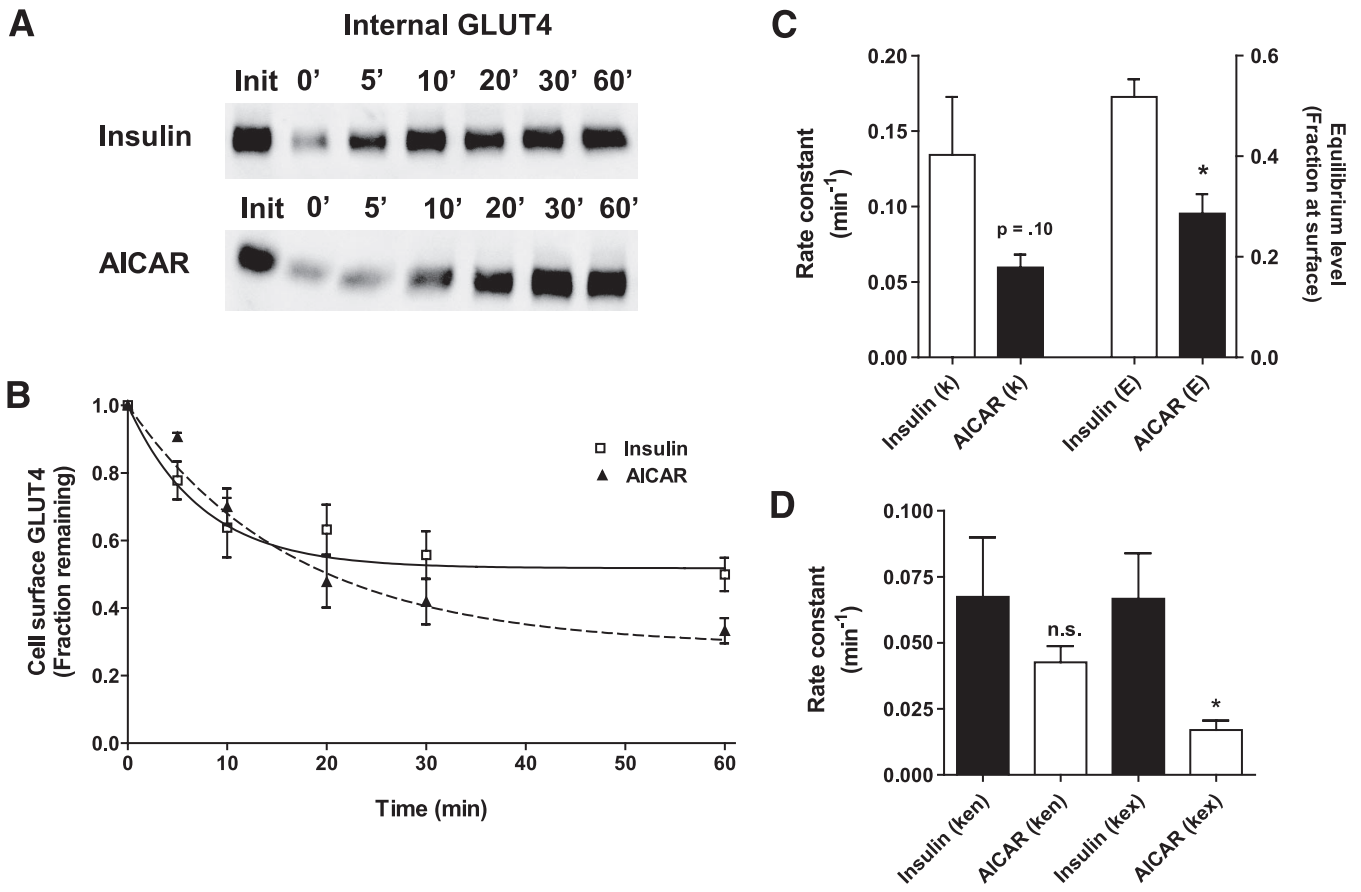

FIG. 3. Internalization of GP15-tagged GLUT4 under steady-state stimulation with insulin or AICAR in rat epitrochlearis muscle. Muscle strips were incubated with 120 nmol/l insulin or 1 mmol/l AICAR and then labeled with GP15. The GP15-tagged GLUT4 was then allowed to internalize for the indicated times. To separately identify internalized GLUT4, avidin was added to the medium to quench the signal from cell surface–located GLUT4. Internal GLUT4 was then solubilized, and the biotin-tagged GLUT4 was precipitated on immobilized streptavidin, resolved on SDS-PAGE gels, and detected and quantified by immunoblot analysis with a GLUT4 antibody. *A*: Representative blots. init, initial labeling without avidin addition. *B*: By comparison of the initial GLUT4 signal with the signal at the indicated times, the level of cell-surface GLUT4 was calculated. *C* and *D*: Curve fitting to data from separate experiments was used to calculate rate constants as described in RESEARCH DESIGN AND METHODS. The curves in *B* were computed from the average rate constants in *C*. Results are the means ± SE of four experiments. *$P < 0.05$.

GP15-GLUT4 to be internalized, and this was found to be adequate (Fig. 4*A*).

The movement of GLUT4 from the internal compartment to the plasma membrane was rendered unidirectional by the addition of avidin at the cell exterior throughout the time course used to study the exocytosis. As the GLUT4 reaches the cell surface, its signal is quenched by avidin binding. The GLUT4 signal that remains in the cell, therefore, represents the fraction of GLUT4 remaining internally, and this decreases with time (Fig. 4*A*). This allows curve fitting to a single exponential function even when the scatter in the data points is quite large (Fig. 4*B*). The scatter is an unavoidable consequence of working with single muscle samples for each time course data point. Insulin treatment increases the rate constant for exocytosis sixfold (0.010 in the basal state to 0.067 min^{-1} in the insulin-stimulated state; $P < 0.05$). However, AICAR treatment does not significantly increase the apparent exocytosis rate constant. The rate constant is 0.012 min^{-1}, which is close to the basal value. This exocytosis rate constant is in reasonable agreement with the steady-state exocytosis rate constant in AICAR-treated cells (0.017 min^{-1}).

A limitation of the fitting of a single exponential function is that it assumes that the internal GLUT4 signal decreases continuously to zero. However, it may not (29,30). In the basal and AICAR-treated cells, the release of GLUT4 may occur in a pulse and the internal GLUT4 signal may reach a plateau point at which no further release occurs. Thus, AICAR may stimulate a portion of the internal GLUT4 to be released. The fitting method we have employed may lead to an underestimate of the rate constant for this partial release. Unfortunately, the data are insufficiently precise for further analysis of this possibility. The more limited exocytosis response to AICAR cannot be due to a slow onset in AMPK activation, as we have compared basal and AICAR at times of exocytosis up to 120 min. Furthermore, the steady-state parameters were obtained following an extensive treatment with AICAR. Taking into consideration both the steady-state and the direct exocytosis measurements, we cannot exclude the possibility of an AICAR-mediated increase in exocytosis; however, this effect is clearly smaller, or more limited as a pulse of release of GLUT4, than that occurring in insulin-treated muscle.

Exocytosis of GLUT4 in insulin- and AICAR-stimulated human vastus lateralis muscle. The exocytosis approach characterized in the isolated rat epitrochlearis muscle system was applied to human muscle strips. We confirmed that the reversal procedure adopted for the rat epitrochlearis was also applicable to human muscle (Fig. 2*B*). A comparison of basal and insulin-treated muscle

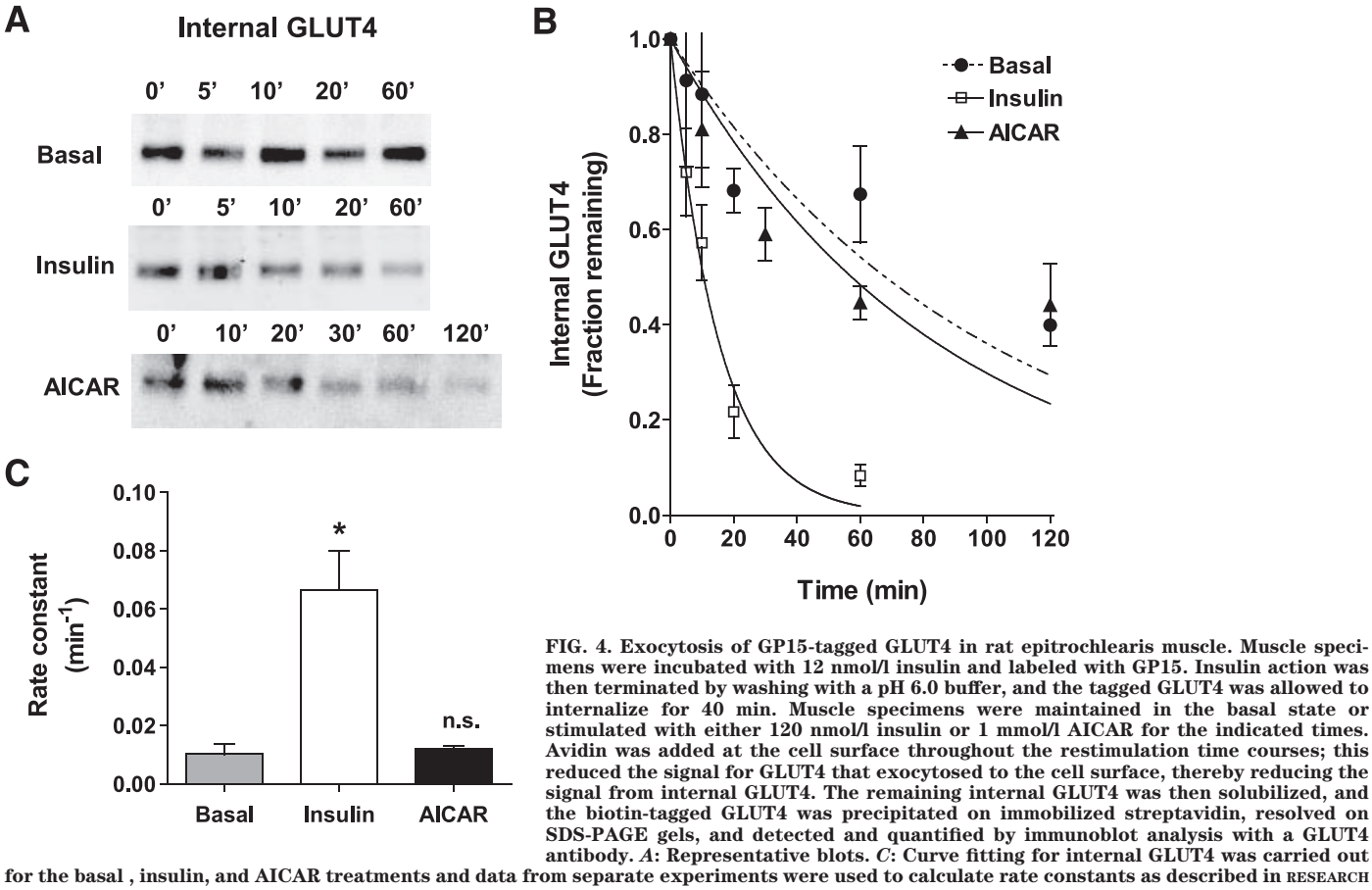

FIG. 4. Exocytosis of GP15-tagged GLUT4 in rat epitrochlearis muscle. Muscle specimens were incubated with 12 nmol/l insulin and labeled with GP15. Insulin action was then terminated by washing with a pH 6.0 buffer, and the tagged GLUT4 was allowed to internalize for 40 min. Muscle specimens were maintained in the basal state or stimulated with either 120 nmol/l insulin or 1 mmol/l AICAR for the indicated times. Avidin was added at the cell surface throughout the restimulation time courses; this reduced the signal for GLUT4 that exocytosed to the cell surface, thereby reducing the signal from internal GLUT4. The remaining internal GLUT4 was then solubilized, and the biotin-tagged GLUT4 was precipitated on immobilized streptavidin, resolved on SDS-PAGE gels, and detected and quantified by immunoblot analysis with a GLUT4 antibody. *A*: Representative blots. *C*: Curve fitting for internal GLUT4 was carried out for the basal , insulin, and AICAR treatments and data from separate experiments were used to calculate rate constants as described in RESEARCH DESIGN AND METHODS. *B*: The curves were computed from the average rate constants in *C*. Results are means ± SE. Data are derived from seven, five, and three experiments for basal, insulin, and AICAR treatments, respectively. Basal experiments had at least three time points, but these were varied to allow comparison with early and late time points for the insulin or AICAR stimulations. **P* < 0.05.

revealed clear insulin stimulation in the GP15-tagged GLUT4 movement out of the internal compartment and toward the cell surface (Fig. 5*A*). Curve-fitting analysis (Fig. 5*B*) and analysis of separate experiments (Fig. 5*C*) revealed that the exocytosis rate constant was increased six- to sevenfold (from 0.011 to 0.075 min^{-1}). These rate-constant values and the six- to sevenfold stimulation are very similar to the changes occurring in rat epitrochlearis muscle. This suggests that the same kinetic process is present, even under conditions in which the levels of glucose transport are quite different. The six- to sevenfold increase in glucose transport activity does not occur in human muscle, but this is not necessarily inconsistent with a large change in GLUT4 translocation, as additional factors may influence the glucose transport activity. The effect of AICAR on GLUT4 exocytosis in human muscle is less clear, partly because of the large scatter in data points derived from the samples available in the study (Fig. 5*B*). Calculation of the exocytosis rate constants (0.017 min^{-1}, Fig. 5*C*) indicated that there may be some slight, but statistically insignificant, stimulation of exocytosis above basal levels following AICAR treatment of the muscle strips. The observed exocytosis rate constant is, however, identical to that derived from the steady-state exocytosis experiment in AICAR-treated rat muscle.

DISCUSSION

Analysis of the trafficking kinetic data parameters for GLUT4 translocation in skeletal muscle is essential to resolve the site of convergence with the insulin-signaling steps. If the site of insulin action is more fully resolved, this would help define where defects in GLUT4 traffic occur in insulin-resistant states and type 2 diabetes. By applying and extending use of our GLUT4-labeling technique, we have provided some of the first evidence that GLUT4 exocytosis in rat and human skeletal muscle is the major site of insulin action and that the magnitude of the stimulation of the exocytosis rate constant is sufficient to account for the observed insulin stimulation of glucose transport.

Studies on relatively simpler cell-culture systems have revealed that GLUT4 traffics through multiple compartments (31,32). In skeletal muscle, additional complexities in the trafficking route occur because of the large fibrous cell structures and the presence of a more complex transverse-tubule network of membranes. Recent studies on green fluorescent protein–tagged GLUT4 in skeletal muscle have highlighted the importance of the transverse-tubule system and have led to the hypothesis that GLUT4 is not translocated over long distances in skeletal muscle but is recruited from GLUT4 satellite compartments localized close to the transverse tubules (17,18). Our photolabeling approach is complementary to studies on GFP-GLUT4, because we tag endogenous GLUT4, rather than expressed recombinant protein. However, the approach does not provide information on any potential differences in trafficking at the sarcolemma or the transverse tubules. Previous autoradiography studies using a tritiated version of a GLUT4 photolabel have provided evidence that the label does penetrate and label GLUT4 in the transverse-

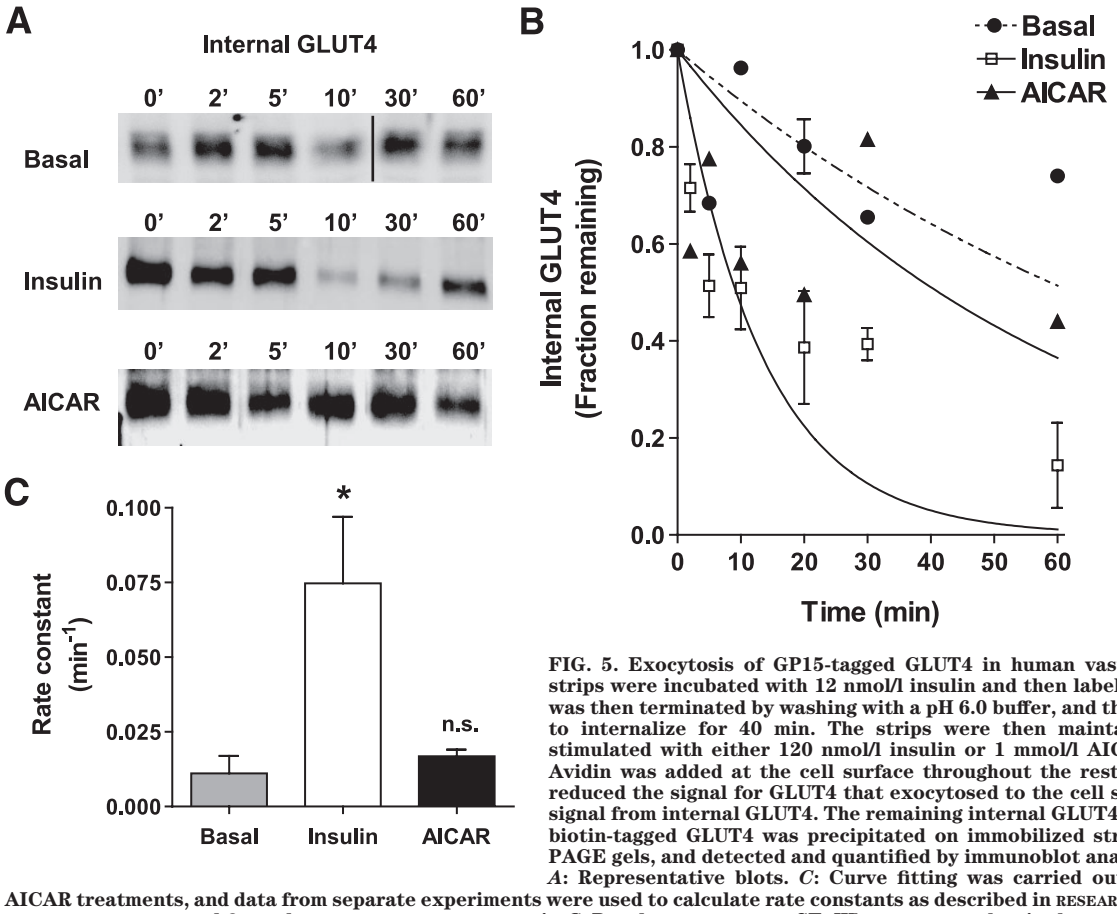

FIG. 5. Exocytosis of GP15-tagged GLUT4 in human vastus lateralis muscle. Muscle strips were incubated with 12 nmol/l insulin and then labeled with GP15. Insulin action was then terminated by washing with a pH 6.0 buffer, and the tagged GLUT4 was allowed to internalize for 40 min. The strips were then maintained in the basal state or stimulated with either 120 nmol/l insulin or 1 mmol/l AICAR for the indicated times. Avidin was added at the cell surface throughout the restimulation time courses; this reduced the signal for GLUT4 that exocytosed to the cell surface, thereby reducing the signal from internal GLUT4. The remaining internal GLUT4 was then solubilized and the biotin-tagged GLUT4 was precipitated on immobilized streptavidin, resolved on SDS-PAGE gels, and detected and quantified by immunoblot analysis with a GLUT4 antibody. *A*: Representative blots. *C*: Curve fitting was carried out for the basal, insulin, and AICAR treatments, and data from separate experiments were used to calculate rate constants as described in RESEARCH DESIGN AND METHODS. *B*: The curves were computed from the average rate constants in *C*. Results are means ± SE. Where no error bar is shown, $n = 2$. Data are derived from four, four, and two experiments for basal, insulin, or AICAR treatment, respectively. In basal experiments, time points were varied to allow comparison with early and late time points for the insulin and AICAR stimulations. *$P < 0.05$.

tubule locations in skeletal muscle (33). Additionally, molecules as large as a fragment antigen binding of an antibody can permeate into transverse-tubule spaces in heart muscle (34).

The six- to sevenfold stimulation of the GLUT4 exocytosis rate in the present study is greater than the fold stimulation of glucose transport. This effect is consistent with data on cell-surface GLUT4 labeling in rat (35) and human (12) skeletal muscle. This may occur because glucose transport is dependent on additional transporters such as GLUT1 that respond less effectively to insulin. Changes in GLUT4 endocytosis and storage will also influence the level of stimulation of transport activity. The absolute values of the rate constants obtained from rat (0.01 for basal and 0.067 min^{-1} for insulin at 30°C) and human (0.011 and 0.075 min^{-1} at 37°C) skeletal muscle studies are remarkably close to adipose cell studies. For example, basal and insulin-stimulated rate constants for GLUT4 exocytosis in 3T3-L1 adipocytes are 0.01 and 0.09 min^{-1}, respectively, at 37°C (27). When the GP15 photolabel in rat adipocytes was used, slightly higher values were obtained (23). The similarity of these rate constants suggests that the same fundamental process rate limits GLUT4 movement in these diverse systems and that this process is relatively unaltered by divergent cell architecture and membrane tubule complexities in these differing cell types.

Our studies on the AICAR compound are less clear. There are several technical problems associated with its use, including its slow onset of action. Even when GLUT4 exocytosis is studied over 120 min, there is no clear evidence that this process is stimulated. In cardiac myocytes, AMPK activation following hypoxia, mitochondrial inhibition (36), or metformin treatment (37) is associated with a reduction in GLUT4 endocytosis. Mitochondrial inhibition and a combination of AICAR treatment and PKC stimulation also lead to inhibition of GLUT4 internalization in L6 muscle cells (38). We find that the initial rate of net internalization and endocytosis of GLUT4 in rat skeletal muscle is also reduced, but these changes do not reach statistical significance. The reduction in net internalization that is evident at early time points is masked in the steady-state experiments by the progress to a lower equilibrium level for the equilibration of the GP15-tagged GLUT4 during AICAR treatment. The endocytosis of GLUT4 is always a more difficult kinetic parameter to obtain and interpret than the unidirectional exocytosis parameter. This is because internalization is a net process, involving both endocytosis and re-exocytosis, and some recycling of GLUT4 will inevitably occur. These limitations may account for some of the controversies that surround the issue of whether insulin markedly reduces GLUT4 endocytosis (16,39,40).

Whether the observed 50% reduction in GLUT4 net internalization is sufficient to account for the full magnitude of the AICAR stimulation of glucose transport (a two- to threefold stimulation) is incompletely resolved in this study. The slow onset of the increase in glucose transport is also consistent with a slowing of GLUT4 endocytosis. Our data suggest that a single site of convergence of

AMPK- and Akt-signaling pathways on a single intermediate such as AS160 (7,41–43) cannot fully and simultaneously account for regulation of GLUT4 traffic at the level of both exocytosis and endocytosis. Indeed, AS160 action is reported to be localized to the exocytosis rather than the endocytosis arm of GLUT4 traffic (40).

The steady-state recycling experiments are of interest and mechanistic importance because they show that in muscle, GLUT4 continues to recycle in both the insulin- and AICAR-stimulated states. In contrast to earlier (44,45), but not later, versions of the translocation hypothesis (13), GLUT4 is not released as a transitory pulse to the cell surface where it would then be resident while the stimulus remains. Instead, GLUT4 continues to recycle even when the stimulus is maintained (13,27). However, the observed recycling could be consistent with a variant of the pulse model in which GLUT4 is released in a pulse from a reservoir compartment to the cell surface and then on to the endosome system, within which it continues to recycle while the stimulus remains (29,30).

In conclusion, our demonstration that exocytosis is the major site of insulin action on GLUT4 traffic in rat and human skeletal muscle suggests that a focus on this limb of the GLUT4 traffic pathway in insulin-resistant conditions such as type 2 diabetes will be necessary and appropriate to resolve defects in glucose metabolism in future studies. Because of the technical challenges and limitations described above, the photolabeling approach will only give a partial and incomplete analysis in future studies. Nevertheless, the approach described is complementary to more dynamic studies in which GLUT4 is analyzed at a detailed subcellular level (18).

ACKNOWLEDGMENTS

This work was supported by grants from the Medical Research Council (U.K.), the Wellcome Trust, the European Foundation for the Study of Diabetes, the Swedish Research Council, the Swedish Diabetes Association, the Strategic Research Foundation, the Knut and Alice Wallenberg Foundation, the Finnish Cultural Foundation and Commission of the European Communities (contract nos. LSHM-CT-2004-005272 EXGENESIS and LSHM-CT-2004-512013 EUGENE2), the European Research Council, the Finnish Academy of Science, the Finnish Diabetes Research Foundation, and the Sigrid Juselius Foundation.

This study also received grant support from the Novo Nordisk Research Foundation. No other potential conflicts of interest relevant to this article were reported.

REFERENCES

1. Defronzo RA, Gunnarsson R, Bjorkman O, Olsson M, Wahren J: Effects of insulin on peripheral and splanchnic glucose metabolism in noninsulin-dependent (type 2) diabetes mellitus. *J Clin Invest* 76:149–155, 1985
2. Eriksson J, Koranyi L, Bourey R, Schalin-Jantti C, Widen E, Mueckler M, Permutt AM, Groop LC: Insulin resistance in type 2 (non-insulin-dependent) diabetic patients and their relatives is not associated with a defect in the expression of the insulin-responsive glucose transporter (GLUT-4) gene in human skeletal muscle. *Diabetologia* 35:143–147, 1992
3. Cline GW, Petersen KF, Krssak M, Shen J, Hundal RS, Trajanoski Z, Inzucchi S, Dresner A, Rothman DL, Shulman GI: Impaired glucose transport as a cause of decreased insulin-stimulated muscle glycogen synthesis in type 2 diabetes. *N Engl J Med* 341:240–246, 1999
4. Shulman GI, Rothman DL, Jue T, Stein P, Defronzo RA, Shulman RG: Quantitation of muscle glycogen synthesis in normal subjects and subjects with non-insulin-dependent diabetes by 13C nuclear magnetic resonance spectroscopy. *N Engl J Med* 322:223–228, 1990
5. Kahn BB, Rosen AS, Bak JF, Andersen PH, Damsbo P, Lund S, Pedersen O: Expression of GLUT1 and GLUT4 glucose transporters in skeletal muscle of humans with insulin-dependent diabetes mellitus: regulatory effects of metabolic factors. *J Clin Endocrinol Metab* 74:1101–1109, 1992
6. Krook A, Roth RA, Jiang XJ, Zierath JR, Wallberg-Henriksson H: Insulin-stimulated Akt kinase activity is reduced in skeletal muscle from NIDDM subjects. *Diabetes* 47:1281–1286, 1998
7. Karlsson HK, Zierath JR, Kane S, Krook A, Lienhard GE, Wallberg-Henriksson H: Insulin-stimulated phosphorylation of the Akt substrate AS160 is impaired in skeletal muscle of type 2 diabetic subjects. *Diabetes* 54:1692–1697, 2005
8. Karlsson HK, Ahlsen M, Zierath JR, Wallberg-Henriksson H, Koistinen HA: Insulin signaling and glucose transport in skeletal muscle from first-degree relatives of type 2 diabetic patients. *Diabetes* 55:1283–1288, 2006
9. Kim YB, Peroni OD, Aschenbach WG, Minokoshi Y, Kotani K, Zisman A, Kahn CR, Goodyear LJ, Kahn BB: Muscle-specific deletion of the Glut4 glucose transporter alters multiple regulatory steps in glycogen metabolism. *Mol Cell Biol* 25:9713–9723, 2005
10. Katz LD, Glickman MG, Rapoport S, Ferrannini E, Defronzo RA: Splanchnic and peripheral disposal of oral glucose in man. *Diabetes* 32:675–679, 1983
11. Koistinen HA, Galuska D, Chibalin AV, Yang J, Zierath JR, Holman GD, Wallberg-Henriksson H: 5-amino-imidazole carboxamide riboside increases glucose transport and cell-surface GLUT4 content in skeletal muscle from subjects with type 2 diabetes. *Diabetes* 52:1066–1072, 2003
12. Ryder JW, Yang J, Galuska D, Rincón J, Björnholm M, Krook A, Lund S, Pedersen O, Wallberg-Henriksson H, Zierath JR, Holman GD: Use of a novel impermeable biotinylated photolabeling reagent to assess insulin- and hypoxia-stimulated cell surface GLUT4 content in skeletal muscle from type 2 diabetic patients. *Diabetes* 49:647–654, 2000
13. Satoh S, Nishimura H, Clark AE, Kozka IJ, Vannucci SJ, Simpson IA, Quon MJ, Cushman SW, Holman GD: Use of bismannose photolabel to elucidate insulin-regulated GLUT4 subcellular trafficking kinetics in rat adipose cells: evidence that exocytosis is a critical site of hormone action. *J Biol Chem* 268:17820–17829, 1993
14. Koumanov F, Jin B, Yang J, Holman GD: Insulin signaling meets vesicle traffic of GLUT4 at a plasma-membrane-activated fusion step. *Cell Metab* 2:179–189, 2005
15. Bai L, Wang Y, Fan J, Chen Y, Ji W, Qu A, Xu P, James DE, Xu T: Dissecting multiple steps of GLUT4 trafficking and identifying the sites of insulin action. *Cell Metab* 5:47–57, 2007
16. Huang S, Lifshitz LM, Jones C, Bellve KD, Standley C, Fonseca S, Corvera S, Fogarty KE, Czech MP: Insulin stimulates membrane fusion and GLUT4 accumulation in clathrin coats on adipocyte plasma membranes. *Mol Cell Biol* 27:3456–3469, 2007
17. Lauritzen HP, Ploug T, Prats C, Tavare JM, Galbo H: Imaging of insulin signaling in skeletal muscle of living mice shows major role of T-tubules. *Diabetes* 55:1300–1306, 2006
18. Lauritzen HP, Galbo H, Brandauer J, Goodyear LJ, Ploug T: Large GLUT4 vesicles are stationary while locally and reversibly depleted during transient insulin stimulation of skeletal muscle of living mice: imaging analysis of GLUT4-enhanced green fluorescent protein vesicle dynamics. *Diabetes* 57:315–324, 2008
19. Sakamoto K, Goodyear LJ: Invited review: intracellular signaling in contracting skeletal muscle. *J Appl Physiol* 93:369–383, 2002
20. Zierath JR: In vitro studies of human skeletal muscle: hormonal and metabolic regulation of glucose transport. *Acta Physiol Scand Suppl* 626:1–96, 1995
21. Wallberg-Henriksson H, Zetan N, Henriksson J: Reversibility of decreased insulin-stimulated glucose transport capacity in diabetic muscle with in vitro incubation: insulin is not required. *J Biol Chem* 262:7665–7671, 1987
22. Chibalin AV, Yu M, Ryder JW, Song XM, Galuska D, Krook A, Wallberg-Henriksson H, Zierath JR: Exercise-induced changes in expression and activity of proteins involved in insulin signal transduction in skeletal muscle: differential effects on insulin-receptor substrates 1 and 2. *Proc Natl Acad Sci U S A* 97:38–43, 2000
23. Yang J, Hodel A, Holman GD: Insulin and isoproterenol have opposing roles in the maintenance of cytosol pH and optimal fusion of GLUT4 vesicles with the plasma membrane. *J Biol Chem* 277:6559–6566, 2002
24. Hashimoto M, Yang J, Holman GD: Cell-surface recognition of biotinylated membrane proteins requires very long spacer arms: an example from glucose transporter probes. *Chembiochem* 2:52–59, 2001
25. Miyamoto L, Toyoda T, Hayashi T, Yonemitsu S, Nakano M, Tanaka S, Ebihara K, Masuzaki H, Hosoda K, Ogawa Y, Inoue G, Fushiki T, Nakao K: Effect of acute activation of 5′-AMP-activated protein kinase on glycogen regulation in isolated rat skeletal muscle. *J Appl Physiol* 102:1007–1013, 2007
26. Holman GD, Karim AR, Karim B: Photolabeling of erythrocyte and

adipocyte hexose transporters using a benzophenone derivative of bis(D-mannose). *Biochim Biophys Acta* 946:75–84, 1988
27. Yang J, Holman GD: Comparison of GLUT4 and GLUT1 subcellular trafficking in basal and insulin-stimulated 3T3–L1 cells. *J Biol Chem* 268:4600–4603, 1993
28. Calderhead DM, Kitagawa K, Tanner LI, Holman GD, Lienhard GE: Insulin regulation of the two glucose transporters in 3T3–L1 adipocytes. *J Biol Chem* 265:13800–13808, 1990
29. Govers R, Coster AC, James DE: Insulin increases cell surface GLUT4 levels by dose dependently discharging GLUT4 into a cell surface recycling pathway. *Mol Cell Biol* 24:6456–6466, 2004
30. Muretta JM, Romenskaia I, Mastick CC: Insulin releases Glut4 from static storage compartments into cycling endosomes and increases the rate constant for Glut4 exocytosis. *J Biol Chem* 283:311–323, 2008
31. Holman GD, Leggio LL, Cushman SW: Insulin-stimulated GLUT4 glucose transporter recycling: a problem in membrane-protein subcellular trafficking through multiple pools. *J Biol Chem* 269:17516–17524, 1994
32. Blot V, McGraw TE: Molecular mechanisms controlling GLUT4 intracellular retention. *Mol Biol Cell* 19:3477–3487, 2008
33. Dudek RW, Dohm GL, Holman GD, Cushman SW, Wilson CM: Glucose-transporter localization in rat skeletal muscle: autoradiographic study using ATB-[3-H]-BMPA photolabel. *FEBS Lett* 339:205–208, 1994
34. Fazakerley DJ, Scott SP, Lizunov VA, Cushman SW, Holman GD: A common trafficking route for GLUT4 translocation in cardiomyocytes following insulin, contraction and energy-status signaling. *J Cell Sci* 122:727–734, 2009
35. Lund S, Holman GD, Schmitz O, Pedersen O: Glut4 content in the plasma membrane of rat skeletal muscle: comparative studies of the subcellular fractionation method and the exofacial photolabelling technique using ATB-BMPA. *FEBS Lett* 330:312–318, 1993
36. Yang J, Holman GD: Insulin and contraction stimulate exocytosis, but increased AMP-activated protein kinase activity resulting from oxidative metabolism stress slows endocytosis of GLUT4 in cardiomyocytes. *J Biol Chem* 280:4070–4078, 2005
37. Yang J, Holman GD: Long-term metformin treatment stimulates cardiomyocyte glucose transport through an AMP-activated protein kinase-dependent reduction in GLUT4 endocytosis. *Endocrinology* 147:2728–2736, 2006
38. Antonescu CN, Diaz M, Femia G, Planas JV, Klip A: Clathrin-dependent and independent endocytosis of glucose transporter 4 (GLUT4) in myoblasts: regulation by mitochondrial uncoupling. *Traffic* 9:1173–1190, 2008
39. Blot V, McGraw TE: GLUT4 is internalized by a cholesterol-dependent nystatin-sensitive mechanism inhibited by insulin. *EMBO J* 25:5648–5658, 2006
40. Zeigerer A, McBrayer MK, McGraw TE: Insulin stimulation of GLUT4 exocytosis, but not its inhibition of endocytosis, is dependent on RabGAP AS160. *Mol Biol Cell* 15:4006–4415, 2004
41. Sakamoto K, Holman GD: Emerging role for AS160/TBC1D4 and TBC1D1 in the regulation of GLUT4 traffic. *Am J Physiol Endocrinol Metab* 295:E29–E37, 2008
42. Treebak JT, Glund S, Deshmukh A, Klein DK, Long YC, Jensen TE, Jorgensen SB, Viollet B, Andersson L, Neumann D, Wallimann T, Richter EA, Chibalin AV, Zierath JR, Wojtaszewski JF: AMPK-mediated AS160 phosphorylation in skeletal muscle is dependent on AMPK catalytic and regulatory subunits. *Diabetes* 55:2051–2058, 2006
43. Cartee GD, Wojtaszewski JF: Role of Akt substrate of 160 kDa in insulin-stimulated and contraction-stimulated glucose transport. *Appl Physiol Nutr Metab* 32:557–566, 2007
44. Cushman SW, Wardzala LJ: Potential mechanism of insulin action on glucose transport in the isolated rat adipose cell: apparent translocation of intracellular transport systems to the plasma membrane. *J Biol Chem* 255:4758–4762, 1980
45. Simpson IA, Yver DR, Hissin PJ, Wardzala LJ, Karnieli E, Salans LB, Cushman SW: Insulin-stimulated translocation of glucose transporters in the isolated rat adipose cells: characterization of subcellular fractions. *Biochim Biophys Acta* 763:393–407, 1983